

UNCLASSIFIED

Defense Technical Information Center  
Compilation Part Notice

ADP012589

TITLE: High Luminescence Efficiency from GaAsN Layers Grown by MBE with RF Nitrogen Plasma Source

DISTRIBUTION: Approved for public release, distribution unlimited

This paper is part of the following report:

TITLE: Progress in Semiconductor Materials for Optoelectronic Applications Symposium held in Boston, Massachusetts on November 26-29, 2001.

To order the complete compilation report, use: ADA405047

The component part is provided here to allow users access to individually authored sections of proceedings, annals, symposia, etc. However, the component should be considered within the context of the overall compilation report and not as a stand-alone technical report.

The following component part numbers comprise the compilation report:  
ADP012585 thru ADP012685

UNCLASSIFIED

## High Luminescence Efficiency from GaAsN Layers Grown by MBE with RF Nitrogen Plasma Source.

Victor M. Ustinov, Nikolai A. Cherkashin, Nikolai A. Bert, Andrei F. Tsatsul'nikov, Alexei R. Kovsh<sup>1\*</sup>, Jyh-Shang Wang<sup>1</sup>, Li Wei<sup>1</sup>, and Jim Y. Chi<sup>1</sup>

A.F.Ioffe Physico-Technical Institute, St.Petersburg 194021, Russia

<sup>1</sup>Industrial Technology Research Institute, Hsinchu 310, Taiwan, R.O.C.

on leave from A.F.Ioffe Physico Technical Institute

### ABSTRACT

(In)GaAsN based heterostructures have been found to be promising candidates for the active region of 1.3 micron VCSELs. However, (In)GaAsN bulk layers and quantum wells usually demonstrate lower photoluminescence intensity than their nitrogen-free analogues. Defects associated with lower temperature growth and N-related defects due to plasma cell operation and possible nonuniform distribution of nitrogen enhance the non-radiative recombination in N-contained layers. We studied the photoluminescence intensity of GaAsN layers as a function of N content in MBE grown samples using rf-plasma source. Increasing the growth temperature to as high as 520 °C in combination with the increase in the growth rate allowed us to avoid any N-related defects up to 1.5% of nitrogen. Low-temperature-growth defects can be removed by post-growth annealing. We achieved the same radiative efficiency of GaAsN samples grown at 520 °C with that of reference layer of GaAs grown at 600 °C. Compositional fluctuations in GaAsN layers lead to characteristic S-shape of temperature dependence of photoluminescence peak position and this feature is the more pronounced the higher the amount of nitrogen in GaAsN. Annealing reduces compositional fluctuations in addition to the increase in the photoluminescence intensity. The results obtained are important for further improving the characteristics of InGaAsN lasers emitting at 1.3 micron.

### INTRODUCTION

Group-III nitride semiconductors are an area of great current interest for the development of lasers and light emitting diodes emitting in the visible to blue and UV ranges. On the other hand, addition of a small amount of nitrogen to GaAs can drastically reduce the band gap towards the infrared region [1]. This is due to the strong bowing of the energy gap in the GaAs-GaN system [2]. The large lattice mismatch between GaAs and GaN (about 21%) limits the composition range of GaAsN pseudomorphically grown on GaAs to only a few percent. The addition of In to GaAsN can lead to strain compensation, and a further decrease in the band gap of the quaternary solid solution can be obtained [3]. However, the growth of InGaAsN layers and quantum well structures of device quality appears to be a challenge even when the amount of nitrogen is less than 3 percent [4]. This is usually enough to achieve emission at 1.3 micron, which is the goal for applications in fiber optic communication systems. 1.3 micron edge-emitting lasers and VCSELs have been recently demonstrated by several research groups [5-8], however, the device characteristics are still basically inferior to those based on InGaAsP and are to be further improved. The advantage of the GaAs/InGaAsN system for laser applications is the use of well-developed AlGaAs/GaAs GRINSCH design where only active region is replaced on pseudomorphically grown InGaAsN/GaAs quantum wells. Therefore, to improve laser performance, one has to improve the quality of the nitrogen containing active region. It has been

shown previously that the nitrogen concentration, growth temperature and post-growth annealing affect the radiation efficiency of GaAsN. In addition, the specific source of nitrogen installed in the growth chamber can play a role, since, e.g., ions coming from a radio-frequency plasma source can damage the growth surface leading to the formation of additional defects. In the present work we show that the optimization of the growth regimes allows us to achieve the luminescence efficiency of  $\text{GaAs}_{1-x}\text{N}_x$  very close to that of GaAs up to  $x=0.015$ . We also study in detail the luminescence properties of our GaAsN epilayers and we argue that the S-shape of the peak position vs temperature dependence frequently observed for InGaAsN/GaAs heterostructures can be considered as the figure of merit of uniformity of nitrogen distribution.

## EXPERIMENT

The samples under investigation were grown in a Riber Epineat apparatus with solid cells for group III elements and arsenic and UNI Bulb RF Plasma Source (Applied EPI) for nitrogen. The 0.2- $\mu\text{m}$ -thick layer (GaAsN or GaAs) was sandwiched by AlGaAs/GaAs superlattices. This design prevents the leakage of non-equilibrium carriers from active layer towards the substrate and the surface and allows us to have the same effective pumping for photoluminescence (PL) studies. The nitrogen composition of the samples was evaluated by x-ray diffraction. Room temperature PL measurements were carried out using a frequency doubled YAG:Nd laser ( $\lambda=532\text{ nm}$ ). Temperature and excitation density dependences of PL were recorded under Ar+ laser excitation ( $\lambda=514.5\text{ nm}$ ). Absorption spectra were extracted from transmission measurements.

## RESULTS AND DISCUSSION

### Effect of growth temperature and growth rate

In agreement with the other published data and the predictions of our thermodynamic calculations [9] we have found that the sticking coefficient of nitrogen is temperature independent over the range of 400-530  $^{\circ}\text{C}$  and decreases at higher temperatures. Therefore, we used the same characteristics of RF plasma source in this temperature interval to have equal nitrogen content for GaAsN provided the growth rate was fixed. At growth temperatures below 550  $^{\circ}\text{C}$  the 2x4 reconstruction of the pattern of reflection high-energy electron diffraction (RHEED) was observed both for GaAs and GaAsN. However, when the substrate temperature was higher than 550  $^{\circ}\text{C}$ , a 3x3 RHEED pattern was observed for the GaAsN growth. It was shown that such RHEED pattern corresponds to the formation of N-rich surface [10].

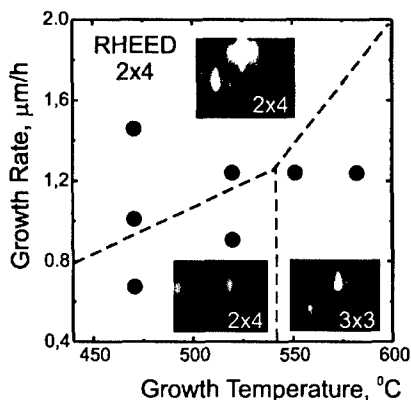


Fig. 1. Growth temperature — growth rate phase diagram for the GaAsN growth. Points indicate samples grown at given growth rate and temperature. RHEED pattern pictures were taken in the  $[1\bar{1}0]$  azimuth.

the growth rate. When the growth rate gets lower than a certain value the growth changes from two-dimensional to three-dimensional. We observed a steep deterioration of optical and structural properties along with this transition. The value of minimum growth rate depends on the growth temperature. These data are presented in Fig. 1 as a growth temperature vs growth rate phase diagram. The upper region corresponds to normal GaAs-like growth mode characterized by high PL intensity. We believe that the reason for the strong decrease in luminescence efficiency for the bottom two regions is associated with additional defects due to either the formation of N-rich clusters or the nitrogen segregation. Thus, there is some region of high "growth rate/growth temperature" that is free of the effects related to the phase separation. We have found that the border of top and bottom regions shifts left (or up) for higher N content. Adding even three percent of indium to match lattice parameter to GaAs also shifts the border about 40 °C left. Therefore, the presence of In enhances phase separation regardless of strain compensation.

### Photoluminescence intensity of GaAs and GaAsN layers

Fig. 2a shows PL spectra (dotted lines) of  $\text{GaAs}_{1-x}\text{N}_x$  layers grown at different growth temperatures, 470 and 520 °C. The luminescence intensity is about one order of magnitude higher for the samples grown at 520 °C. One can see that increasing the nitrogen content leads to the red shift of PL line. Integrated luminescence intensity is nearly constant for  $x=0-0.015$  and falls about three times for  $x=0.024$  (circles). PL intensity of GaAs layers also strongly depends on growth temperature (diamonds). The highest intensity shows the sample grown at 600 °C which is about one order of magnitude higher than that of the sample grown at 520 °C and 50 times higher than of the sample grown at 470 °C. It is important to note that the PL intensity of

GaAs samples grown at 520 and 470 °C is very close to that of the  $\text{GaAs}_{1-x}\text{N}_x$  samples ( $x<0.015$ ). Fig. 2(b) shows the dependence of integrated PL intensity on excitation density measured with an Ar-laser. Data for a GaAs sample grown at 600 °C are also shown. The PL intensities are almost the same for the two samples grown at 520 °C even for very low power densities. It proves that nitrogen incorporation does not lead to formation of additional centers of non-radiative recombination. Thus, the main reason for decreasing PL intensity for GaAsN layers relative to the reference GaAs sample grown at optimal temperature 600 °C is low temperature growth rather than the presence of nitrogen.

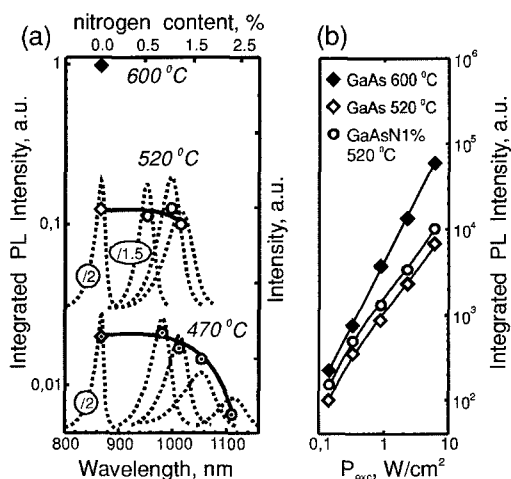


Fig.2. (a)–Dependence of integrated PL intensity of GaAs(N) layers on wavelength grown at different temperatures (left axis). PL spectra of GaAs(N) layers are shown as dotted lines (right axis).

(b)–Dependence of integrated PL intensity on excitation power density for GaAs and GaAsN.

## Effect of annealing

It is well known that defects related to low-temperature growth, such as arsenic antisite and/or interstitial defects, can be removed by post-growth annealing. We have investigated the effect of *in situ* annealing on our GaAsN layers. We found that the increase in luminescence intensity after annealing varied from 3 to 50 times depending on the growth temperature, Fig.3. The solid horizontal line shows intensity of GaAs grown at 600 °C, which is considered to be an optimal growth temperature for GaAs. Again one can see that PL intensity depends on growth temperature but not on the presence of N in the layers. PL intensity of samples after annealing is shown by open circles. For samples grown at 520 °C and annealed for 1 hour at 750 °C under arsenic overpressure we achieved almost the same PL intensity as GaAs grown at 600 °C.

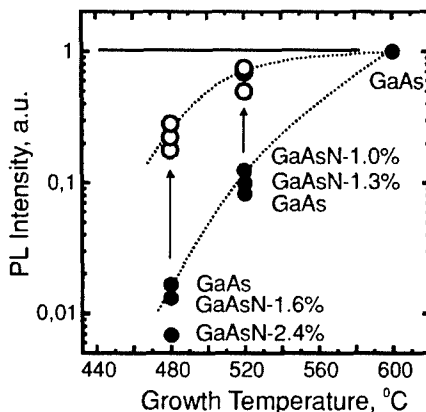


Fig.3 Dependence of integrated PL intensity of GaAs(N) layers as grown and after annealing.

## Structural and optical properties of GaAsN layers

We have shown that to avoid clusterization and realize two-dimensional growth at high growth temperature ( $>500$  °C) one can use relatively high growth rate ( $>1$   $\mu\text{m}/\text{hour}$ ). PL (solid line) and absorption (dotted line) spectra of the  $\text{GaAsN}_{0.01}$  layer grown under this condition are presented in Fig.4. Insert in Fig. 4 shows cross section of transmission electron microscopy image of this sample. One can see that there is no evidence of strong compositional modulations in GaAsN layer. However, pronounced Stokes shift between the maximum of PL spectrum and absorption edge indicates that carrier recombination goes via some localized states.

Photoluminescence spectra taken at low excitation density ( $0.6 \text{ W}/\text{cm}^2$ ) in the 10-300K range are shown in Fig. 5(a). One can see that after 100 K an additional high-energy peak (E2) appears in the spectrum and starts to dominate at higher temperatures. The temperature dependence of the positions of these low-energy (E1) and high-energy-peaks (E2) is shown in Fig. 5(b) by up-triangles and down-triangles, respectively. Only one peak at all temperatures is observed for PL spectra recorded at high excitation ( $100 \text{ W}/\text{cm}^2$ ). Its position and absorption edge are also presented in Fig. 5(b) as solid circles and diamonds, respectively. The PL peak maximum at high excitation is close to E1 at low temperature and shifts towards E2 when the temperature is increased. Finally, at temperatures higher than 70K all data coalescence into one. The characteristic S-shape temperature dependence of the peak position is clearly seen. This S-shape temperature dependence of PL peak position after post-growth annealing is considerably less pronounced (open circles in Fig. 5(b)). To investigate the reason for this S-shaped temperature dependence, we have studied PL temperature dependences of two nominally

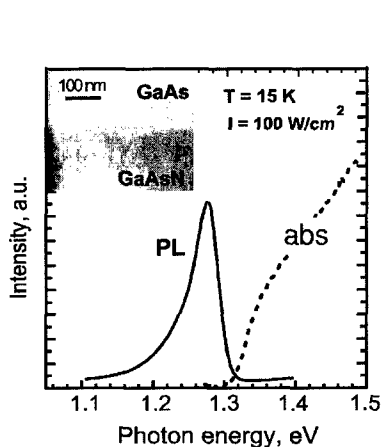


Fig.5. PL (solid line) and absorption spectra (dotted line) of  $\text{GaAsN}_{0.01}$ . Insertion shows TEM image.

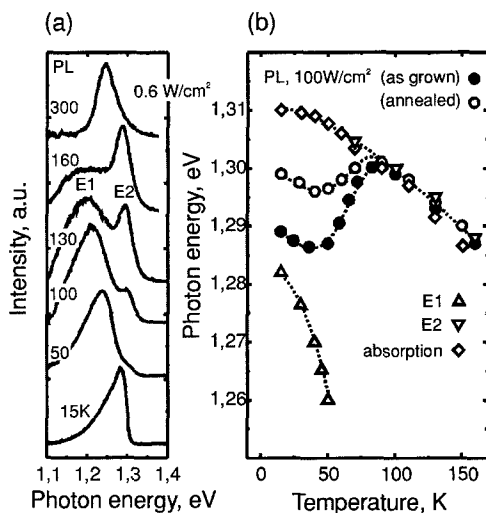


Fig.6. (a) PL spectra of  $\text{GaAsN}_{0.01}$  at different temperatures. (b) Dependence of PL peak position PL, E1 and E2 peaks, and absorption edge.

identical InGaAs QW structures grown under different growth regimes. Conventional structure with flat interfaces demonstrated usual temperature dependence of PL line following the GaAs bandgap. The structure with pronounced interface corrugation, grown under reduced As flux showed double peaked shape of the PL line and the peak intensities redistributed with the observation temperature. Fig. 6.

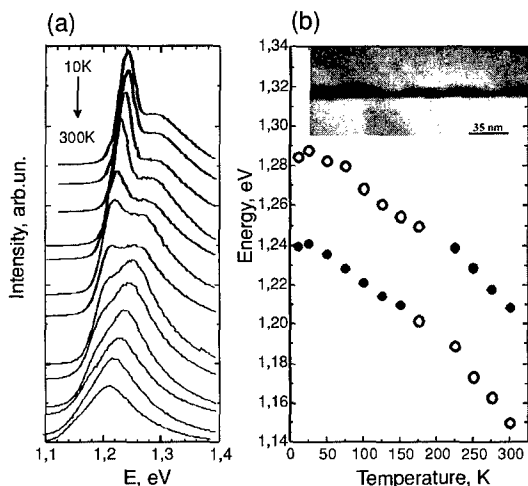


Fig.6(a)- PL spectra of corrugated InGaAs QW at different temperatures. (b) Temperature dependence of position of both PL peaks. Position of peak dominated in PL is shown as circles.

Thus, the main peak shows practically the same S-shape dependence as the GaAsN epilayers described above. Since the two InGaAs QW structures differ only in the interface corrugation leading to additional potential fluctuations we conclude that the main reason for the S-shaped temperature dependence of the PL line is potential fluctuations due to spatial nonuniformities or composition/strain modulations. Therefore, we attribute the S-shape behavior of temperature dependence of PL line in GaAsN epilayers to potential fluctuations due to nonuniformities of nitrogen distribution. Post-growth annealing reduces these inhomogeneities and the S-shape behavior becomes less pronounced. We note that these nonuniformities in nitrogen distribution are not revealed in TEM, so the shape of temperature dependence of PL line can be considered as empirical figure of merit for the extent of uniformity of nitrogen distribution in GaAsN layers.

## CONCLUSIONS

Molecular beam epitaxial growth of  $\text{GaAs}_{1-x}\text{N}_x$  layers has been studied as a function of nitrogen content and growth regimes. We have found that the growth at relatively high growth temperatures allows us to avoid "phase separation" or clusterization if high ( $>1 \mu\text{m/h}$ ) growth rates are used. Up to 1.5% of nitrogen can be incorporated into GaAs without deterioration of integrated PL intensity, and for a sample containing 2.4% of nitrogen the integrated PL intensity decreases only about three times. Such layers demonstrate some compositional fluctuations leading to S-shape temperature dependence of the PL peak position. Annealing reduces compositional fluctuations and improves photoluminescence intensity.

## ACKNOWLEDGEMENTS

This work is supported by the Ioffe-ITRI Joint Scientific Program. The work in Ioffe Institute was also partly supported by the NATO Science for Peace Program (grant SFP-972484).

## REFERENCES

1. M. Weyers and M. Sato, *Appl. Phys. Lett.*, **62**, 1396-1398 (1993).
2. S-H- Wei and A. Zunger, *Phys. Rev. Lett.*, **76**, 664-667 (1996).
3. M. Kondow, K. Uomi, A. Niwa, A. Kitatani, S. Watahiki, and Y. Yazawa, *Japan. J. Appl. Phys.*, **35**, 1273-1275 (1996).
4. H. P. Xin and C. W. Tu, *Appl. Phys. Lett.*, **72**, 2442-2444 (1998).
5. A. Yu. Egorov, D. Bernklau, D. Livshits, V. Ustinov, Zh. I. Alferov, and H. Riechert, *Electron. Lett.*, **35**, 1643-1644 (1999).
6. M. Kawaguchi, E. Gouardes, D. Schlenker, T. Kondo, T. Miyamoto, F. Koyama, and K. Iga, *Electron. Lett.*, **36**, 1776-1777 (2000).
7. G. Steinle, H. Riechert, and A. Yu. Egorov, *Electron. Lett.*, **37**, 93-95 (2001).
8. A. W. Jackson, R. L. Naone, M. J. Dalberth, K. J. Malone, D. W. Kisker, J. F. Klem, K. D. Choquette, D. K. Serkland, and K. M. Geib, *Electron. Lett.*, **37**, 355-356 (2001).
9. V. A. Odnoblyudov, A. Yu. Egorov, A. R. Kovsh, A. E. Zhukov, N. A. Malcev, E. S. Semenova, and V. M. Ustinov, *Semicond. Sci. Technol.*, **16**, 831-835 (2001).
10. R. J. Hauenstein, D. A. Collins, X. P. Cai, M. L. O'Steen, T. C. McGill, *Appl. Phys. Lett.*, **66**, 2861 (1995).